Available online at www.sciencedirect.com

ScienceDirect

IFAC PapersOnLine 51-4 (2018) 681–686

An Improved Frequency-domain Method for the Fractional Order $PI^{\lambda}D^{\mu}$ Controller Optimal Design

Weijia Zheng * **Ying Luo** ** **Yangquan Chen** *** **Youguo Pi** ****
Wei Yu †

* *School of Automation, Foshan University, Foshan, China, (e-mail: z.wj08@mail.scut.edu.cn)*
** *School of Automation, Foshan University, Foshan, China, (e-mail: luoyinglarry@gmail.com)*
*** *School of Engineering, University of California, Merced, 5200 North Lake Road, Merced, CA, USA*
**** *School of Automation Science and Engineering, South China University of Technology, Guangzhou, China*
† *School of Automation, Foshan University, Foshan, China*

Abstract: An improved frequency-domain design method is proposed to design the fractional order $PI^{\lambda}D^{\mu}$ controller. Using this improved method, the parameters of the fractional order $PI^{\lambda}D^{\mu}$ controllers can be obtained immediately according to the model characteristics and design specifications. A proportional relation between the integral gain and derivative gain is built, while the derivative order is set to be equal to the integral order. The proportional coefficient between integral gain and derivative gain is studied and modeled based on priori knowledge and data fitting, and then the estimation model for the optimal proportional coefficient is built. The proposed tuning method is applied to design a fractional order $PI^{\lambda}D^{\mu}$ controller for a permanent magnet synchronous motor servo system. Motor speed control simulations are performed to verify the proposed method. Simulation results show that the obtained control system can achieve robustness and the optimized step response performance.

Keywords: PID control, fractional order controller, frequency-domain method, feedback control, data fitting

1. INTRODUCTION

The proportional integral derivative (PID) control is the most widely used control method in the industrial control area. In recent years, fractional calculus has aroused interest and attention of scholars (Podlubny (1999a), Monje et al. (2010), Luo et al. (2010), Luo and Chen (2009)). The fractional order proportional integral derivative ($PI^{\lambda}D^{\mu}$) controller has the potential to achieve better control performance over the traditional PID controller because the adjustable integral order λ and derivative order μ are introduced, expanding the control scope of the controller (Podlubny (1999b)). However, on the other hand, the tuning of the $PI^{\lambda}D^{\mu}$ controller is more complicated.

The tuning methods of fractional order PI^{λ}/D^{μ} controller can mainly be divided into two kinds, the frequency-domain design method (Luo et al. (2010), Luo and Chen (2009)) and the optimization methods (Biswas et al. (2009), Zheng and Pi (2016)). The frequency-domain method is often applied to design the fractional order PI^{λ} or PD^{μ} controller. Based on the given gain crossover frequency and phase margin, the controller parameters are calculated according to the gain robustness specification. The obtained control system achieves reliable stability and the robustness to gain variations. However, as discussed in this paper, this method cannot be directly applied to tune the fractional order $PI^{\lambda}D^{\mu}$ controller.

A tuning method based on the differential evolution (DE) algorithm is proposed (Zheng et al. (2017)), satisfying the specifications in both frequency-domain and time-domain simultaneously. The obtained control system achieves the optimal dynamic performance, while the frequency-domain design requirements are also satisfied. However, applying this method, large amount of space and time are spent in the numerical optimization. Therefore, this method may not be suitable for engineering application.

An improved frequency-domain design method is proposed to design the fractional order $PI^{\lambda}D^{\mu}$ controller in this paper. In order to reduce the pending parameters of the controller, the proportional relation between the integral gain K_i and derivative gain K_d is built, while the derivative order μ is set to be equal to the integral order λ. Based on this modification, the number of the pending parameters is reduced from five to three. Therefore, the current frequency-domain design method can be applied to tune the fractional order $PI^{\lambda}D^{\mu}$ controller. The proportional coefficient between K_i and K_d is studied and modeled based on priori knowledge and data fitting, and then the estimation model for the optimal proportional coefficient

10.1016/j.ifacol.2018.06.180

is built. The proposed tuning method is applied to design a fractional order PI$^\lambda$D$^\mu$ controller for a permanent magnet synchronous motor (PMSM) servo system. Motor speed control simulations are performed and the advantage of the improved frequency-domain method is demonstrated.

2. IMPROVED FREQUENCY-DOMAIN DESIGN METHOD

The fractional order PI$^\lambda$D$^\mu$ controller is described by (1),

$$C(s) = K_p\left(1 + \frac{K_i}{s^\lambda} + K_d s^\mu\right), \tag{1}$$

where K_p, K_i and K_d are proportional, integral and derivative gains, respectively; λ and μ are the fractional orders.

Based on (1), the amplitude and phase of the controller are obtained as described by (2) and (3),

$$|C(j\omega)| = K_p\sqrt{P(\omega)^2 + Q(\omega)^2}, \tag{2}$$

$$\mathrm{Arg}[C(j\omega)] = \arctan\left(\frac{Q(\omega)}{P(\omega)}\right), \tag{3}$$

where

$$P(\omega) = 1 + K_i\omega^{-\lambda}\cos\left(\frac{\pi}{2}\lambda\right) + K_d\omega^\mu\cos\left(\frac{\pi}{2}\mu\right), \tag{4}$$

$$Q(\omega) = K_d\omega^\mu\sin\left(\frac{\pi}{2}\mu\right) - K_i\omega^{-\lambda}\sin\left(\frac{\pi}{2}\lambda\right). \tag{5}$$

The plant model for controller design has the form represented by (6),

$$G(s) = \frac{K}{s^3 + \tau_1 s^2 + \tau_2 s}. \tag{6}$$

Based on (6), the amplitude and phase of the plant model are obtained as described by (7) and (8),

$$|G(j\omega)| = \frac{K}{\sqrt{A(\omega)^2 + B(\omega)^2}}, \tag{7}$$

$$\mathrm{Arg}[G(j\omega)] = -\arctan\left(\frac{B(\omega)}{A(\omega)}\right), \tag{8}$$

where

$$A(\omega) = -\tau_1\omega^2, B(\omega) = \tau_2\omega - \omega^3. \tag{9}$$

Based on the frequency-domain design method, the control system should be robust to the loop-gain variations. According to the robustness specification, the derivative of the phase-frequency curve is zero, namely, the phase Bode plot is flat at the gain crossover frequency. For the plant model $G(s)$ and controller $C(s)$, the loop-gain robustness equation is then described by (10),

$$\left.\frac{d[\mathrm{Arg}[G(j\omega)C(j\omega)]]}{d\omega}\right|_{\omega=\omega_c} = 0, \tag{10}$$

where ω_c is the given gain crossover frequency, satisfying

$$|G(j\omega_c)C(j\omega_c)| = 1. \tag{11}$$

To ensure the stability of the control system, the phase margin φ_m is also given, satisfying

$$\mathrm{Arg}[G(j\omega_c)] + \mathrm{Arg}[C(j\omega_c)] = -\pi + \varphi_m. \tag{12}$$

The fractional order PI$^\lambda$D$^\mu$ controller has five parameters to be tuned, K_p, K_i, K_d, λ and μ. However, only three equations are derived from the design specifications. Therefore, the current frequency-domain design method cannot be applied to tune the fractional order PI$^\lambda$D$^\mu$ controller directly.

A modification on the current design method is proposed to solve this problem. The proportional relation between the integral gain K_i and derivative gain K_d is built, as described by (13),

$$K_d = aK_i, \tag{13}$$

where a is the proportional coefficient. Besides, the derivative order μ is set to be equal to the integral order λ. Therefore, the modified fractional order PI$^\lambda$D$^\mu$ controller is described by (14),

$$C(s) = K_p\left(1 + \frac{K_i}{s^\lambda} + aK_i s^\lambda\right). \tag{14}$$

Substituting (14) into (12), K_i can be represented as (15),

$$K_i = \frac{-M}{M{\omega_c}^{-\lambda}cos(\frac{\lambda\pi}{2}) + aM{\omega_c}^{\lambda}cos(\frac{\lambda\pi}{2}) + aN{\omega_c}^{\lambda}sin(\frac{\lambda\pi}{2}) - N{\omega_c}^{-\lambda}sin(\frac{\lambda\pi}{2})}, \tag{15}$$

where

$$M = A(\omega_c)tan(-\pi + \varphi_m) + B(\omega_c), \tag{16}$$

$$N = B(\omega_c)tan(-\pi + \varphi_m) - A(\omega_c). \tag{17}$$

Similarly, substituting (14) into (10), the equation about K_i is obtained, as described by (18),

$$Q_2{K_i}^2 + Q_1K_i + Q_0 = 0, \tag{18}$$

where

$$Q_2 = \frac{2a\lambda}{\omega_c}sin(\lambda\pi) + 2aQ_0cos(\lambda\pi) + a^2Q_0{\omega_c}^{2\lambda} + \frac{Q_0}{{\omega_c}^{2\lambda}}, \tag{19}$$

$$Q_1 = \frac{a\lambda}{{\omega_c}^{1-\lambda}}sin(\frac{\lambda\pi}{2}) + \frac{\lambda}{{\omega_c}^{\lambda+1}}sin(\frac{\lambda\pi}{2}) + 2aQ_0{\omega_c}^{\lambda}cos(\frac{\lambda\pi}{2}) + \frac{2Q_0}{{\omega_c}^{\lambda}}cos(\frac{\lambda\pi}{2}), \tag{20}$$

$$Q_0 = \frac{d[\mathrm{Arg}[G(j\omega)]]}{d\omega}\Big|_{\omega=\omega_c}. \tag{21}$$

According to the frequency-domain method, the gain crossover frequency ω_c and the phase margin φ_m are given in advance. Therefore, for a specific plant model $G(s)$, once the coefficient a between K_i and K_d is determined, K_i and λ can be calculated based on (15) and (18). Then K_d and μ can also be obtained. Finally, K_p can be calculated according to (11). Thus, all the parameters of the fractional order PI$^\lambda$D$^\mu$ controller are obtained.

3. ESTIMATION MODEL OF THE PROPORTIONAL COEFFICIENT

According to the improved frequency-domain method, the proportional coefficient a between K_i and K_d should be determined before the controller parameters are calculated. Therefore, the dynamic performance of the control system is significantly affected by the value of a. To ensure good dynamic performance of the obtained control system, the estimation model of a is needed to be built.

The estimation model of a is built based on the following assumption. For a plant model $G(s)$ and a specific (ω_c, φ_m) setting, an optimal fractional order PI$^\lambda$D$^\mu$ controller can be derived from the optimal value of a. The distributions of the optimal a corresponding to each (ω_c, φ_m) setting can be approximated by a model related to the (ω_c, φ_m) setting and the plant model characteristics. Furthermore, the approximated model of the optimal a is continuously defined in the hyperspace of ω_c, φ_m and the related model characteristic parameters.

The estimation model of the optimal a is built according to the following steps. First, several test models are built based on the interested model parameter ranges. Similarly, several (ω_c, φ_m) pairs are selected according to the design requirements. Second, the optimal values of a corresponding to different (ω_c, φ_m) pairs and test models are collected. Third, based on the collected data, the distribution rules of the optimal a for different (ω_c, φ_m) settings and model characteristics are studied. Finally, the estimation model of a is built according to the summarized distribution rules.

3.1 Optimal Data Collection

In this paper, the estimation model of the optimal a is built for the PMSM servo system having the form described by (6). According to the commonly used PMSM models, the range of parameter τ_1 is set to be 100 to 140, while that of τ_2 is set to be 8000 to 11000. Besides, in order to satisfy the general design requirement, the range of the given gain crossover frequency ω_c is set to be $35rad/s$ to $60rad/s$, while that of the given phase margin φ_m is set to be 45° to 60° (Ruan et al. (2016)).

Based on the range of τ_1, three values of τ_1: 100, 120 and 140 are selected to build the test models. Similarly, three values of τ_2: 8000, 9500 and 11000 are also selected. The gain K has no influence on the value of a, it is fixed to be 30000. Therefore, nine test models are built by combining the values of τ_1 and τ_2, as described from (22) to (30),

$$G_1(s) = \frac{30000}{s^3 + 100s^2 + 8000s}, \tag{22}$$

$$G_2(s) = \frac{30000}{s^3 + 120s^2 + 8000s}, \tag{23}$$

$$G_3(s) = \frac{30000}{s^3 + 140s^2 + 8000s}, \tag{24}$$

$$G_4(s) = \frac{30000}{s^3 + 100s^2 + 11000s}, \tag{25}$$

$$G_5(s) = \frac{30000}{s^3 + 120s^2 + 11000s}, \tag{26}$$

$$G_6(s) = \frac{30000}{s^3 + 140s^2 + 11000s}, \tag{27}$$

$$G_7(s) = \frac{30000}{s^3 + 100s^2 + 9500s}, \tag{28}$$

$$G_8(s) = \frac{30000}{s^3 + 120s^2 + 9500s}, \tag{29}$$

$$G_9(s) = \frac{30000}{s^3 + 140s^2 + 9500s}. \tag{30}$$

Based on the range of ω_c, seven values of ω_c: $35rad/s$, $37rad/s$, $40rad/s$, $45rad/s$, $50rad/s$, $55rad/s$, $60rad/s$ are selected to tune the controllers. Similarly, four values of φ_m: 45°, 50°, 55°, 60° are also selected.

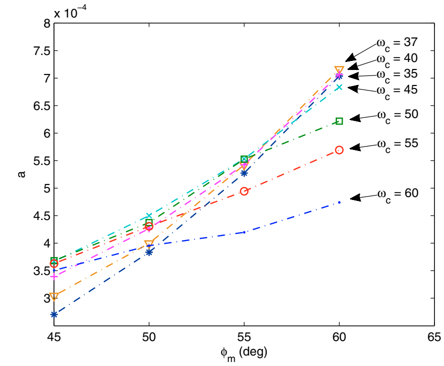

Fig. 1. The distributions of optimal a with regard to φ_m

The integrated time absolute error (ITAE) is selected to be the dynamic performance index of the control system. The ITAE index is described by (31),

$$J = \int_0^\infty t\,|e(t)|\,dt, \tag{31}$$

where $e(t)$ represents the deviation between the expected output and the actual output.

For each test model $G_i(s)$, the optimal values of a are collected following the steps below.

(1) Combine the values of given ω_c and φ_m and then generate the (ω_c, φ_m) groups.
(2) Select 25 values of a uniformly in the range of a, obtaining a_1, a_2, ..., a_{25}.
(3) Calculate the controller parameters based on each a_j ($j = 1, 2, ..., 25$).
(4) Step response simulation is performed and the ITAE of the control system output is calculated.
(5) The value of a with the least ITAE is selected to be the optimal one.

Following these steps, the optimal values of a for nine test models are collected.

3.2 Estimation Model Study

The optimal value of a should be related to the given crossover frequency ω_c, phase margin φ_m and the phase-frequency characteristics of the plant model. First, the relation between the optimal a and the given φ_m is studied, under the condition that the given ω_c is fixed. Taking $G_1(s)$ as an example, the distributions of the optimal a with regard to φ_m are plotted in Fig. 1. Based on Fig. 1, the optimal a satisfies the linear relationship with φ_m when ω_c is fixed. Therefore, the optimal a can be described by (32),

$$a = A\varphi_m + B, \tag{32}$$

where A and B are related to the given gain crossover frequency ω_c and the phase-frequency characteristics of the plant model.

The distributions of the optimal a with regard to φ_m are fitted applying the least square method. Thus, the values of A and B corresponding to different given ω_c for model $G_1(s)$ are obtained. The same process is performed on the

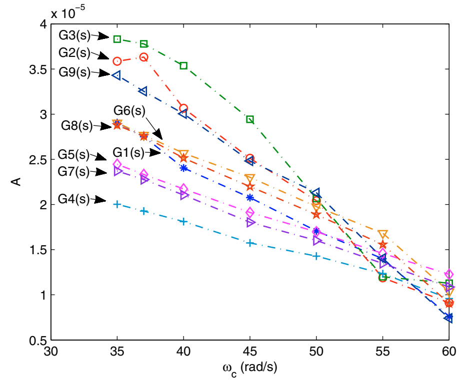

Fig. 2. The distributions of A with regard to ω_c

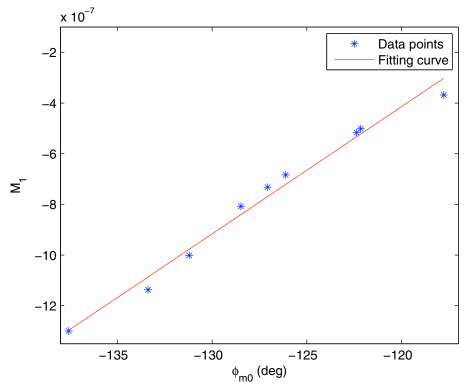

Fig. 3. The distributions of M_1 with regard to φ_{m0}

other eight test models and then the values of A and B for $G_1(s)$ to $G_9(s)$ are obtained. The distributions of A with regard to ω_c for different test models are plotted in Fig. 2. Based on Fig. 2, A approximately satisfies the linear relationship with ω_c. Therefore, A can be described by (33),

$$A = M_1\omega_c + N_1, \tag{33}$$

where M_1 and N_1 are also related to the phase-frequency characteristics of the plant model. The values of M_1 and N_1 are obtained by fitting the distributions of A with regard to ω_c using the least square method. Thus, the values of M_1 and N_1 corresponding to different test models are obtained.

In order to study the distributions of M_1 and N_1 with regard to the phase-frequency characteristics of the plant model, seven frequency points: $35rad/s$, $37rad/s$, $40rad/s$, $45rad/s$, $50rad/s$, $55rad/s$, $60rad/s$ are selected in the gain crossover frequency range. The phases at these frequency points are calculated and the mean phase φ_{m0} within the frequency range is obtained by calculating the average of seven values. Performing such calculations on nine test models, the mean phases corresponding to nine models, $\varphi_{m0}(G_1(s))$, $\varphi_{m0}(G_2(s))$, ..., $\varphi_{m0}(G_9(s))$ are obtained.

The distributions of M_1 with regard to mean phase φ_{m0} are plotted as data points in Fig. 3. Based on Fig. 3, M_1 satisfies the linear relationship with φ_{m0}, as described by (34),

$$M_1 = P_1\varphi_{m0} + Q_1, \tag{34}$$

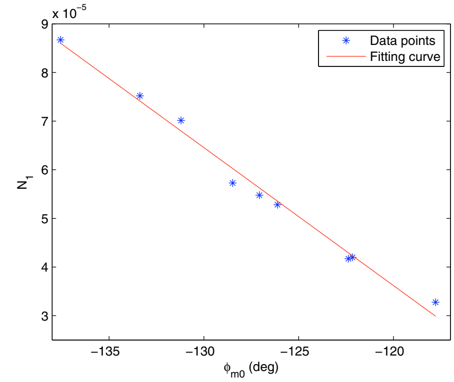

Fig. 4. The distributions of N_1 with regard to φ_{m0}

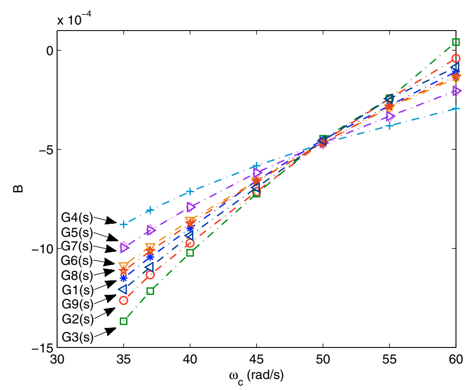

Fig. 5. The distributions of B with regard to ω_c

where P_1 and Q_1 are pending constants. Applying the least square method to fit the distributions of M_1 with regard to φ_{m0}, the values of P_1 and Q_1 are obtained, $P_1 = 5.033 \times 10^{-8}$, $Q_1 = 5.627 \times 10^{-6}$, the fitting line is plotted in red in Fig. 3.

The distributions of N_1 with regard to mean phase φ_{m0} are plotted as data points in Fig. 4. Based on Fig. 4, N_1 satisfies the linear relationship with φ_{m0}, as described by (35),

$$N_1 = P_2\varphi_{m0} + Q_2, \tag{35}$$

where P_2 and Q_2 are pending constants. Applying the least square method to fit the distributions of N_1 with regard to φ_{m0}, the values of P_2 and Q_2 are obtained, $P_2 = -2.838 \times 10^{-6}$, $Q_2 = -3.044 \times 10^{-4}$, the fitting line is plotted in red in Fig. 4.

In order to study the relations between B in (32) and the given ω_c, the distributions of B with regard to ω_c for different test models are plotted in Fig. 5. Based on Fig. 5, B approximately satisfies the linear relationship with ω_c, as described by (36),

$$B = M_2\omega_c + N_2, \tag{36}$$

where M_2 and N_2 are related to the phase-frequency characteristics of the plant model. The values of M_2 and N_2 are obtained by fitting the distributions of B with regard to ω_c using the least square method. Thus, the values of M_2 and N_2 corresponding to different test models are obtained.

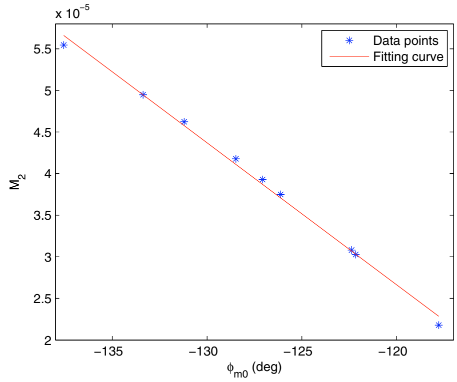

Fig. 6. The distributions of M_2 with regard to φ_{m0}

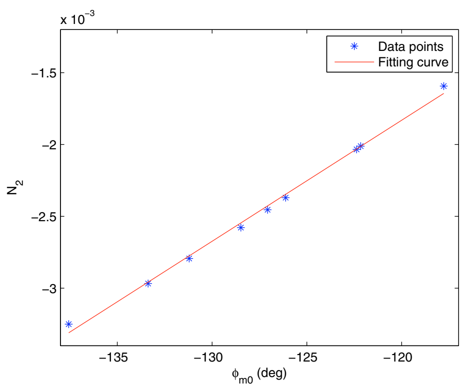

Fig. 7. The distributions of N_2 with regard to φ_{m0}

The distributions of M_2 with regard to mean phase φ_{m0} are plotted as data points in Fig. 6. Based on Fig. 6, M_2 satisfies the linear relationship with φ_{m0}, as described by (37),

$$M_2 = X_1\varphi_{m0} + Y_1, \tag{37}$$

where X_1 and Y_1 are pending constants. Applying the least square method to fit the distributions of M_2 with regard to φ_{m0}, the values of X_1 and Y_1 are obtained, $X_1 = -1.707 \times 10^{-6}$, $Y_1 = -1.782 \times 10^{-4}$, the fitting line is plotted in red in Fig. 6.

In order to study the relations between N_2 and the phase-frequency characteristics of the plant model, the distributions of N_2 with regard to mean phase φ_{m0} are plotted as data points in Fig. 7. Based on Fig. 7, N_2 satisfies the linear relationship with φ_{m0}, as described by (38),

$$N_2 = X_2\varphi_{m0} + Y_2, \tag{38}$$

where X_2 and Y_2 are pending constants. Applying the least square method to fit the distributions of N_2 with regard to φ_{m0}, the values of X_2 and Y_2 are obtained, $X_2 = 8.425 \times 10^{-5}$, $Y_2 = 0.0083$, the fitting line is plotted in red in Fig. 7.

All the parameters of the estimation model are obtained. The estimation model of a is described by (39),

$$\begin{aligned} a &= [(P_1\varphi_{m0}+Q_1)\omega_c+P_2\varphi_{m0}+Q_2]\varphi_m+(X_1\varphi_{m0}+Y_1)\omega_c+X_2\varphi_{m0}+X_2 \\ &= [(0.00000005033\varphi_{m0}+0.000005627)\omega_c-0.000002838\varphi_{m0}-0.0003044]\varphi_m \\ &\quad -(0.000001707\varphi_{m0}+0.0001782)\omega_c+0.00008425\varphi_{m0}+0.0083. \end{aligned} \tag{39}$$

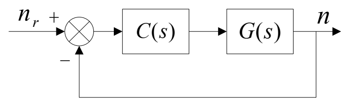

Fig. 8. The PMSM speed closed-loop control system

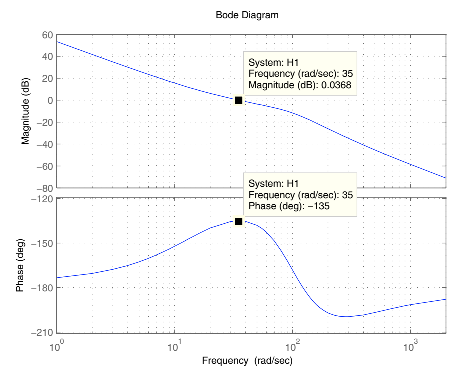

Fig. 9. The open Bode plot of the control system

4. ESTIMATION MODEL APPLICATION

In this section, in order to verify the obtained estimation model, the coefficient a is calculated and the fractional order PI$^\lambda$D$^\mu$ controller is designed for a real PMSM servo system. Besides, given the same ω_c and φ_m, a fractional order PI$^\lambda$ controller is also obtained using the current frequency-domain method. Step response simulations are performed and the dynamic performance of two control systems are compared. The Oustaloup method (Oustaloup (1995), Oustaloup et al. (2000)) is applied to approximate the fractional order operator in the simulation models.

The PMSM speed closed-loop control system is shown in Fig. 8, where $G(s)$ represents the PMSM plant model, $C(s)$ represents the speed controller, n_r represents the reference speed and n represents the speed output.

The transfer function of the PMSM plant model is described by (40),

$$G(s) = \frac{47979.257}{s^3 + 127.38s^2 + 9995.678s}. \tag{40}$$

Given the gain crossover frequency $\omega_c = 35rad/s$, the phase margin $\varphi_m = 45°$, the optimal coefficient a is obtained using (39), $a = 3.185 \times 10^{-4}$. Then the fractional order PI$^\lambda$D$^\mu$ controller is obtained applying the frequency-domain method, as described by (41),

$$C_1(s) = 6.5754\left(1 + \frac{14.7083}{s^{0.9615}} + 0.0047s^{0.9615}\right). \tag{41}$$

The open-loop Bode plot of the control system is shown in Fig. 9. The gain crossover frequency ω_c is $35rad/s$ and the phase margin φ_m is 45°. Besides, the phase characteristic curve is flat at ω_c. Therefore, the design requirements on stability and robustness are satisfied.

In order to check the robustness of the obtained control system, the loop-gain of $C_1(s)$ is set to be 100%, 120% and 80% of its nominal value to simulate the plant model uncertainty. Setting the reference speed n_r to be 1000rpm, the motor speed step response simulations are performed,

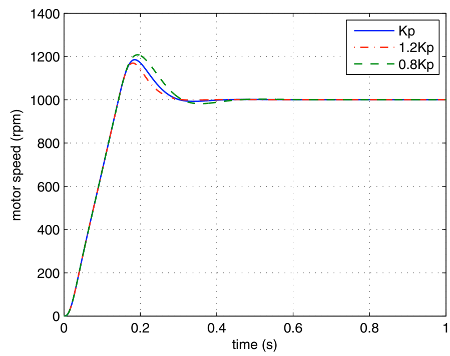

Fig. 10. The step response of the control systems with different loop-gains

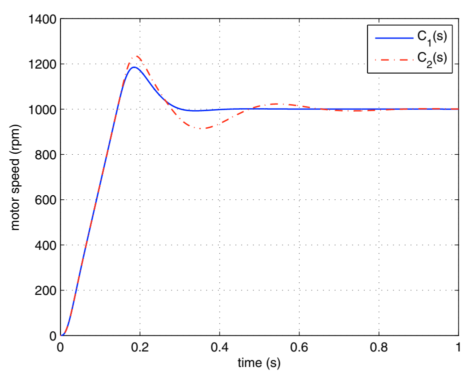

Fig. 11. The step response of two control systems

using the controllers with different gains to control the motor speed. The response curves are shown in Fig. 10.

Based on Fig. 10, the overshoots of the response curves of the control system with different loop-gains are close to each other. Therefore, the control system achieves the robustness to gain variations.

A fractional order PI$^\lambda$ controller is obtained using the current frequency-domain method,

$$C_2(s) = 8.4909\left(1 + \frac{49.1288}{s^{1.4049}}\right). \tag{42}$$

Setting the reference speed n_r to be 1000rpm, the motor speed step response simulation is performed, using $C_1(s)$ and $C_2(s)$ to control the motor speed respectively. The response curves of two control systems are shown in Fig. 11. Based on Fig. 11, the step response using $C_1(s)$ has smaller overshoot and shorter settling time. Therefore, using the coefficient a obtained from the estimation model, the obtained control system achieves better step response performance than that of the system using the PI$^\lambda$ controller obtained from the current frequency-domain method.

Based on the simulation results, the proposed tuning method is valid for the fractional order PI$^\lambda$D$^\mu$ controller design. For any plant model having the form represented by (6), whose parameters are located in the specified ranges, the value of a can be calculated applying the estimation model and then the controller parameters can be obtained applying the frequency-domain method. The obtained control system achieves robustness and the optimized step response performance. Besides, compared with the optimization methods, the tuning procedure of the improved frequency-domain method is straightforward and timesaving, suitable for engineering application.

5. CONCLUSION

An improved frequency-domain design method for fractional order PI$^\lambda$D$^\mu$ controller is proposed. The proportional relation between K_i and K_d is built, while μ is set to be equal to λ. The estimation model of the proportional coefficient between K_i and K_d is built for the commonly used PMSM servo systems. Motor speed step response simulations are performed to verify the estimation model and the proposed tuning method. Simulation results show that the improved frequency-domain design method is valid and the obtained control system can achieve robustness and the optimized step response performance.

REFERENCES

Biswas, A., Das, S., Abraham, A., and Dasgupta, D. (2009). Design of fractional-order PI$^\lambda$D$^\mu$ controllers with an improved differential evolution. *Eng. Appl. Artif. Intel.*, 22(2), 343–50.

Luo, Y. and Chen, Y.Q. (2009). Fractional order [proportional derivative] controller for a class of fractional order systems. *Automatica*, 45(10), 2446–50.

Luo, Y., Chen, Y.Q., Wang, C.Y., and Pi, Y.G. (2010). Tuning fractional order proportional integral controllers for fractional order systems. *J. Process. Contr.*, 20(7), 823–31.

Monje, C., Chen, Y., Vinagre, B., Xue, D., and Feliu-Batlle, V. (2010). *Fractional-order Systems and Controls: Fundamentals and Applications.* Springer, London.

Oustaloup, A. (1995). *La Dérivation Non Entière: Théorie, Synthèse et Applications.* Editions Hermès, Paris.

Oustaloup, A., François, L., Benoît, M., and Florence, M. (2000). Frequency-band complex noninteger differentiator: Characterization and synthesis. *IEEE Transactions on Circuits and SystemsI: Fundamental Theory and Applications*, 47(1), 25–29.

Podlubny, I. (1999a). *Fractional Differential Equations.* Academic Press, New York.

Podlubny, I. (1999b). Fractional-order systems and PI$^\lambda$D$^\mu$ controllers. *IEEE. T. Automat. Contr.*, 44(1), 208–14.

Ruan, Y., Yang, Y., and Chen, B. (2016). *Control Systems of Electric Drives – Motion Control Systems.* China Machine Press, Beijing, 5th edition.

Zheng, W., Luo, Y., Wang, X., Pi, Y., and Chen, Y. (2017). Fractional order PI$^\lambda$D$^\mu$ controller design for satisfying time and frequency domain specifications simultaneously. *ISA. T.*, 68, 212–22.

Zheng, W. and Pi, Y. (2016). Study of the fractional order proportional integral controller for the permanent magnet synchronous motor based on the differential evolution algorithm. *ISA. T.*, 63, 287–93.